Polish J. Chem., **78**, 1103–1119 (2004)

Hydrogen Atom and Hydrogen Ion Interactions with the [100] Surface of Transition Metals (Pd, Ni, Ag, Cu)*

by W.M. Bartczak[1,2], S. Romanowski[2] and J. Stawowska[1]**

[1]*Institute of Radiation Chemistry, Technical University, 93-590 Łódź, Wróblewskiego 15, Poland*
[2]*Department of Theoretical Chemistry, University of Łódź, Łódź, Poland*

(Received March 4th, 2004; revised manuscript June 7th, 2004)

Quantum calculations of interaction of the atomic hydrogen with metal (Pd, Ni, Ag, Cu) clusters with the structure of the fcc [100] surface have been performed. The calculations have been based on the gradient-corrected methods of the Density Functional Theory. For a given position (X,Y) of the hydrogen atom over the metal plane the distance Z from the plane was optimized in order to obtain the highest binding energy which was defined as the difference between the total energy of the H-Me cluster and the energy of the separate H atom and metal cluster. The results of the calculations allowed us to construct the Potential Energy Surfaces for a series of systems. It appears that the H atom binding energy along the valley perpendicular to the metal-metal bond varies only slightly. This suggests easy diffusion of hydrogen along this path. The potential barrier for the hydrogen diffusion over palladium surface is of the order of 0.17 eV. In the case of Ni, Ag and Cu we observe potential barriers with a maximum above the metal-metal bond, with the barrier height 0.68 eV, 0.62 eV and 0.79 eV, respectively. Separate calculations have been performed for the positively charged clusters. For the case of the charged clusters the potential barriers are lower than the value for the neutral clusters. The barriers are 0.27 eV for Ni, 0.35 eV for Ag and 0.58 eV for Cu. For Pd the barrier for the positively charged cluster is 0.5 eV, higher than the value for the neutral case, but for the negatively charged cluster the barrier is practically 0.The results of calculations for all the cases considered suggest the possibility of easy, sometimes activationless, diffusion of hydrogen atoms over the metal surface.

Key words: hydrogen, transition metals, DFT, surface diffusion

A detailed description of the bonding of different atoms and molecules with transition metals is of primary importance to our understanding the processes in which the metals play a role of catalyst. An important model of catalysis is represented by the behaviour of the simplest molecule, H_2, dissociating at the surfaces of the transition and noble metals and their alloys. Subsequent migration of atomic hydrogen over the metal surface and its reactions with atoms or molecules adsorbed on the surface form principal parts of mechanism of numerous catalytic processes.

The literature on catalysis contains a large number of papers on the H atom interaction with metals, mostly Pd, Pt, Ni, Ag and Cu. The book [1] contains useful

---

* Dedicated to Prof. Dr. Z. Galus on the occasion of his 70th birthday.
** Author for correspondence, tel. (48) 426313191, fax (48) 426360246, e-mail: wmb@mitr.p.lodz.pl

review of the older theoretical work. In spite of a large number of theoretical papers on the topic, it is still worth revisiting it. Calculations of electronic properties of transition metals performed by traditional *ab initio* methods were not very successful. An excellent discussion of the results of the calculations of transition metal dimers is given in the Salahub review [2]. Salahub, Morokuma and other authors advocated the use of the density functional theory rather than classical Hartree-Fock schemes. There is a large number of review papers and compilations on this topic and the proceedings of a relatively recent ACS Symposium [3] can serve as a source of references. Significant progress in the transition-metal calculations is connected with the "gradient-corrected" density functionals, sometimes referred to as the nonlocal functionals [4].

Recent years brought a continuous stream of papers which were devoted to the problem of hydrogen adsorption on metals, in particular on palladium. Full citation of all the papers needs probably a separate review. Numerous references are also given in the recent book by Gross which includes a detailed treatment of hydrogen interaction with Pd [5] and in the review paper by Efremenko [6]. A number of authors applied the DFT method with local density approximation and generalized gradient approximation (GGA) and with periodic boundary conditions. For instance Paul and Sautet [7] and Løvvik and Olsen [8] investigated the adsorption of atomic hydrogen on a palladium [111] surface. GGA calculations are also presented in the papers by: Dong and Hafner [9], Ledentu *et al.* [10] and Dong *et al.* [11]. Okuyama and coworkers [12] performed a detailed experimental investigation of hydrogen adsorption at Pd [100] surface and penetration into the bulk of Pd.

Wonchoba and Truhlar [13] reported the binding energy of the hydrogen atom with the Ni [100] surface as –64.76 (kcal/mol) for rather large H–Ni distance of 1.83 Å. The Monte Carlo simulations of Mattsson and coworkers [14] result in the activation energy for the hydrogen diffusion process on Ni [100] equal to 0.12 eV. The same authors [15] calculated the hydrogen adsorption energy –3.38 eV and the potential barrier for diffusion 0.173 eV by the LDA method. The calculations by the GGA method yielded –2.76 eV and 0.127 eV, respectively. The calculations performed by Klinke and Broadbelt [16] for Ni [111] surface using the FP-LAPW (*full-potential linearized augmented planewaves*) method give the following results: –2.05 eV for the binding energy and 1.49 Å for the H–Ni distance for the "*on top*" position, –2.61 eV and 1.62 Å for the "*bridge*" position, –2.89 eV and 1.69 Å for the "*fcc hollow*" position and –2.87 eV and 1.68 Å for the "*hcp hollow*" position. Lee *et al.* [17,18] measured the activation energy for surface diffusion of H atom on the Ni [100]. They reported 1.2 kcal/mol for temperatures 120–160 K, 3.5 kcal/mol for the range 160–200 K. In the range from 108 to 125 K and for Ni [111] surface they suggest the activationless tunnelling mechanism.

In the present paper we investigated the energy surfaces for the H atom interacting with a metal cluster for different positions of the H atom over the fcc elementary cell. As a result we obtained the paths for easy diffusion of the hydrogen atom from cell to cell and we found the energy barriers for the diffusion. The height of

the barrier is of the order of 0.2 eV for the Pd surface, from 0.3 eV to 0.6 eV for Ni and Ag and from 0.6 eV to 0.8 eV for Cu. This results in high mobility of hydrogen atoms over the metal surfaces investigated.

METHODS OF CALCULATIONS

In the present work the quantum calculations of interaction of the atomic hydrogen with metal clusters have been performed. The aim of the project was to compare the results for different versions (and different exchange-correlation functionals) of the DFT calculations and for different metals. The quantum-chemical calculations were performed using the DFT part of the Gaussian98 suite of programs [19]. The gradient-corrected methods of the Density Functional Theory have been applied. The list of the combinations of the gradient-corrected Becke functional for the exchange with different correlation functionals includes: the Perdew-1986 functional, the Perdew-Wang functional and the Lee, Yang and Parr (LYP) functional (see [4] for the detailed description and the references). Using the commonly accepted code words for different functionals (explained, for instance, in the Koch and Holthausen book [4] and in the Gaussian98 help files) we applied the BP86 and the hybrid functionals B3P86, B3LYP, B3PW91. For most of the calculations we used the B3P86 functional. However, some calculations have also been performed for the local SVWN functional. For all the calculations reported here the LANL2DZ double-zeta basis set was used. This is the double-zeta set [20] which includes the Los Alamos effective core potentials due to Hay and Wadt [21].

The calculations of the potential energy surfaces. The calculations reported in this paper correspond to the phase after the H_2 dissociation into the H atoms. We study the system composed of a hydrogen atom and a planar Me_5 metal cluster of the fcc structure ([100] surface). The internuclear distances between the metal atoms are fixed at the positions of the crystal lattice of the metal. The calculations have been performed for a large number of physically different positions (X,Y) of the H atom over the metal cluster. The (X,Y) points were selected inside of the Dirichlet region of the central Pd atom and then the rules of symmetry of the fcc lattice were applied to cover the whole cell. **Thus, outside of the central Dirichlet region the map does not correspond to the real Pd cluster but rather to the fcc lattice cell of the [100] surface.** For a given (X,Y) point we performed the calculations of the energy of $H–Me_5$ system for different heights Z of the H atom above the metal plane and found the Z_{opt} that gives the lowest energy of the system. The calculations were performed for the lowest possible spin states. After subtraction of the energy of the separated Me_5 cluster and H atom we obtain the three-dimensional plot of the H atom binding energy as a function of its (X,Y) position. The plot of $E_b(X,Y,Z_{opt})$ forms the Potential Energy Surface (PES).

RESULTS AND DISCUSSION

Interaction of hydrogen with palladium clusters. Figure 1 shows the results of the calculations for H–Pd system using the B3P86 model. The upper part of the figure shows the three dimensional plot of the H atom binding energy E_b as a function of the (X,Y) coordinates of the hydrogen atom over the Pd surface cell. The unit of X, Y coordinates is 1.945 Å. The lower plot shows the optimized geometry of the H–Pd system: the optimized Z coordinate is plotted as a function of the (X,Y) coordinates: $Z_{opt}(X,Y)$. On the energy surface of Fig. 1 we observe deep valley (marked white and very light grey) where the H atom binding energy is much lower than anywhere else in the cell. The valley is perpendicular to the Pd–Pd bonds and halves the bond. The

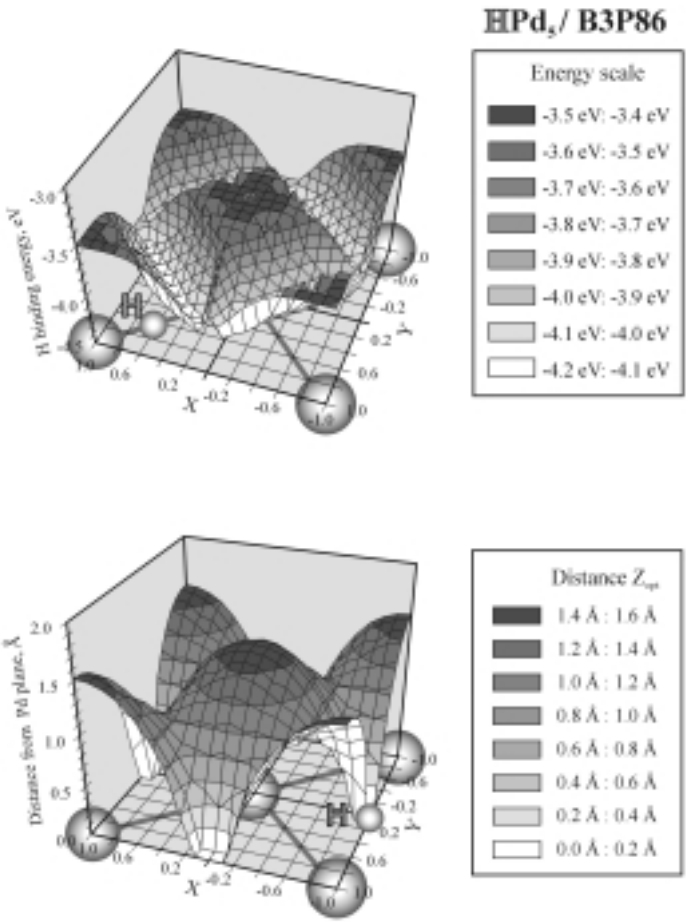

Figure 1. (Upper part) Three-dimensional plot of the binding energy of the single H atom in different positions over the elementary surface cell (fcc [100]) of palladium. (Lower part) A 3-D plot of the optimized distance of the H atom over the Pd cell, Z_{opt}. The unit on the X and Y axis is 1.945 Å. The color coding of the energy and the distance scale is given in the Figure. The calculations have been performed by the DFT/B3P86 method.

crossection of the energy surface along the direction Y = 1-X perpendicular to the bond is given in Fig. 2 together with the plots for different DFT versions and functionals.

The range of the coordinate in the cell is $-1 \leq X \leq 1$. From X = 0.5 (over the Pd–Pd bond centre) up to X = 0.96 (or 0.04 in the other direction) the energy is practically constant. A slight variation in energy, of the order of 0.01 eV, is certainly below the accuracy of the calculations. Between X = 0.96 and X = 1 (or between X = 0.04 and X = 0) the energy increases slightly, by about 0.17 eV. Crossing this barrier means that the H atom is transferred to another surface cell. Hence, the barrier along the line

Y = 1-X can be interpreted as the activation barrier for diffusive movement of the H atoms over the surface of palladium. The activation energy for the H atom diffusive motion at the surface is about 0.17 eV, *i.e*. 3.9 kcal/mol. with the barrier width about 0.08 Å. Both the thermal mechanism and quantum-mechanical tunnelling give very significant probability of the barrier crossing. The Boltzmann factor $\exp(-\Delta E/kT)$ at temperatures 300 K, 600 K i 900 K is 0.0014, 0.037 and 0.11, respectively. The exponential factor in the Gamow formula for the tunnelling probability is 0.9667.

The optimum distance Z of the H atom from the Pd plane (lower part of Figure 1) varies quite significantly over the positions in the cell. The „on top" position (X = 0, Y = 0) is characterized by relatively large distance Z = 1.52 Å. The „on bridge" position (X = 0.5, Y = 0.5) shows a shorter distance Z = 0.98 Å. The movement of the H atom from the „on bridge" point along the Y = 1-X line towards the cell edge is characterized by a steady decrease of the Z distance. In the vicinity of the cell edge (at the top of the barrier, X=0, Y=1) the Z distance falls down to 0 Å. This means that at the foot of the barrier the H atom, which is placed very close to the Pd surface plane, can choose one of the two possible paths: either migrate at the surface crossing the barrier of about 4.0 kcal/mol or migrate under the surface with similar barrier. Okuyama *et al*. [12] estimated the barrier for the subsurface diffusion of the H atom as about 1.1 kcal/mol. Paul and Sautet [7] in their calculations of the hydrogen adsorption on a Pd [111] surface give somewhat different estimations. They obtained 7.6 kcal/mol for the subsurface penetration and roughly estimate 3.5 kcal/mol for the surface diffusion. Due to very low barriers the both paths are possible. Finally, it is worth mentioning that our result for the activation barrier for surface diffusion is very close to the measured activation energy of the H-atom bulk diffusion in Pd which is 5.3 kcal/mol [22].

The binding energy for hydrogen atom as predicted by different DFT models is shown in Figure 2. The figure shows the results for the DFT calculations with gradient-corrected hybrid functionals: B3P86, B3PW91 and B3LYP, for gradient-corrected DFT with the "pure" BP86 functional and for the local DFT with the SVWN (combination of the Slater exchange and Vosko-Wilk-Nusair correlation [4]) functional. The level of the binding energy and the geometry of the surface are slightly different for different methods, but for all the PES surfaces we observe the flat valley perpendicular to the Pd–Pd bond (Y = 1-X) ending with low and narrow energy barrier.

In Figure 2 we compare the energy variation along the line Y = 1-X for different computational models. The different methods result in the shift of the energy plateau at the bottom of the valley but the height of the barrier is roughly the same, of the order of 0.2–0.3 eV. It is interesting to note that the hybrid functionals predict more narrow barrier than the remaining two functionals. However, the general conclusion holds for all the models: **the valley Y = 1-X and its symmetric counterparts provide the easy diffusion path for atomic hydrogen on the palladium surface and the path endings at edge of the Pd cell provide the channels for the H atom penetration beneath the metal surface.**

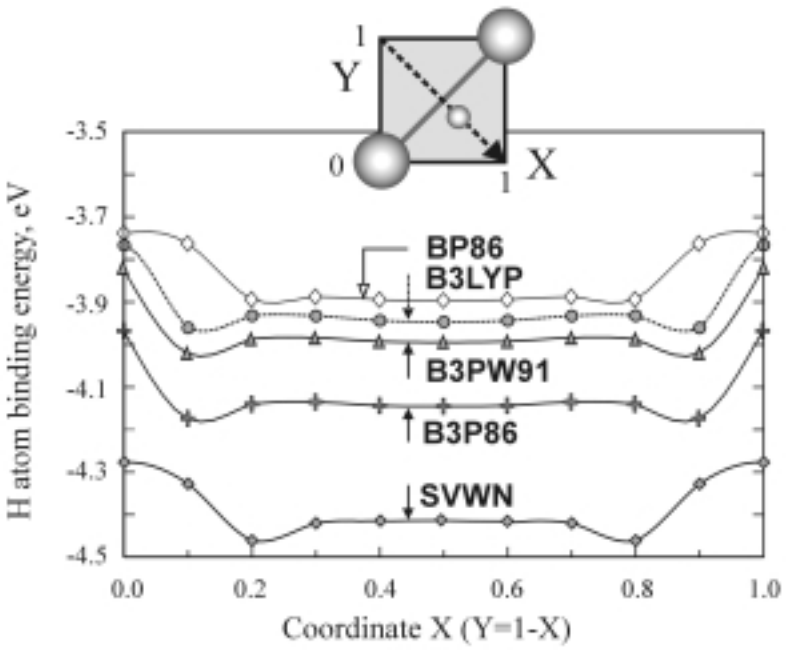

Figure 2. Comparison of the H atom binding energy along the direction Y = 1-X (perpendicular to the Pd–Pd bond) in elementary Pd cell. X axis unit corresponds to 1.945 Å. The calculations were performed using the DFT method with the exchange-correlation functionals as labeled in the figure.

The obvious disadvantage of the calculations shown in Figs. 1, 2 is the planar shape of the metal cluster. To verify the calculations it is necessary to consider the influence of the atoms of the subsurface layer. However, as it was mentioned in the introduction, the calculations of the interaction of adsorbed atoms with the metal transition surface have to be performed by the most advanced methods, preferably the non-local DFT. This, in turn, limits the number of the metal atoms in the cluster to a relatively small number. Therefore we selected such clusters which illustrate the effect of the subsurface atoms but the cost of the calculations is still acceptable.

Figure 3 in the upper part shows the PES for H atom in contact with the cluster denoted as $Pd_4\_Pd_1$ constructed as follows. In the elementary fcc cell the centres of the vertical sides are occupied by the metal atoms. We cut 4 atoms from the surface layer that form the square and one of the subsurface atoms placed under the centre of the square. The geometry of the $Pd_4\_Pd_1$ cluster is shown in the upper part of Figure 3. The Figure presents the binding energy of the H atom in different positions (X,Y) above the metal cluster. The middle part of the Figure shows the fragment of the PES from Figure 1, for the planar Pd_5 cluster, transformed to the coordinate system of the upper figure.

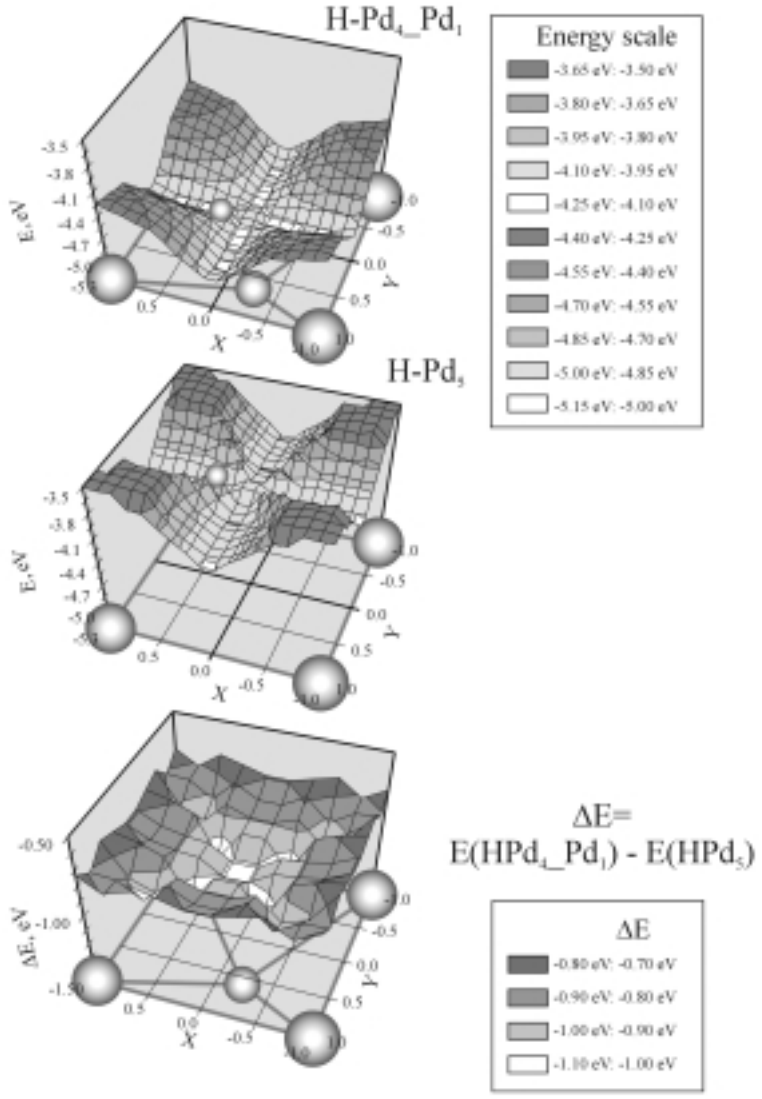

Figure 3. Energy surfaces for H atom binding energy in different positions over the parts of the Pd surface elementary cell. The upper part shows the energy surface for the H atom over the Pd_4_Pd_1 cluster (the structure with one subsurface Pd atom), the middle part shows the energy surface for the planar Pd_5 cluster in the coordinate system of the upper figure. X axis unit corresponds to 1.375 Å. The lower figure shows the energy difference of the surfaces of the upper and middle figure.

The PES of the upper and the middle part of Figure 3 exhibit quite similar geometry. The maximum energy appears at the vortices of the square, directly above the Pd atoms. The valleys of the minimum energy and the paths of easy diffusion of hydrogen atom are placed along the square symmetry axis parallel to the edges.

However, there is significant energy difference between the PES for the $Pd_4\_Pd_1$ and Pd_5 systems. The $H–Pd_4\_Pd_1$ energy surface is shifted down and the shift results from the presence of the subsurface Pd atom. The lower part of the Figure shows the energy difference between the $H–Pd_4\_Pd_1$ and $H–Pd_5$ systems. In the central part of the square, where the influence of the subsurface Pd atom is the most significant, the energy difference is between –1.1 eV and –0.9 eV (–25.37 and –20.75 kcal/mol).

The cross sections of the $H–Pd_4\_Pd_1$ and $H–Pd_5$ surfaces along the square symmetry axis show that our conclusion about easy diffusion of the hydrogen atom is still valid. The $H–Pd_5$ curve has a maximum of 0.17 eV (3.92 kcal/mol) at the centre of the square. The $H–Pd_4\_Pd_1$ plot shows a smaller maximum (0.05 eV or 1.15 kcal/mol) at the centre and slightly higher maximum (0.15 eV or 3.46 kcal/mol) at the square edge. This means that for the both cases the H atom can move along the axis with very small activation barriers and the presence of the subsurface metal atom does not decrease the H atom surface mobility.

The last figure of the Pd series shows the results for the charged structures: H^+ and H^- interacting with the planar Pd cluster. Figure 4 shows the comparison of the PES for $H–Pd_5$ system (upper part), $H^+–Pd_5$ system (middle part) and $H^-–Pd_5$ system (lower part) calculated for the B3P86 functional. The results are rather surprising. The first problem appears when the reference energy level is considered. In the case of the neutral cluster the sum of the energy of isolated H atom and Pd_5 cluster is, of course, the obvious choice. Equally obvious choice of the reference energy for the positively charged cluster is isolated proton H^+ and Pd_5. The Mulliken charge analysis shows however that the H atom at the distance 1.5 Å above Pd has the partial charge +0.19 *e* for the neutral cluster, +0.24 *e* for the positively charged cluster and +0.15 *e* for the negatively charged cluster. The excess charge of hydrogen is delocalized over the metal atoms. For larger distances the partial charge on the hydrogen is very close to 0. Moreover, the sum of energy of the isolated H and Pd_5^+ is by 7.6 eV lower than the sum for isolated H^+ and Pd_5. Similar effect, with 4.1 eV energy difference, was observed for the negatively charged cluster. Hence, the energy of isolated neutral hydrogen and Pd_5^+ or Pd_5^- was assumed as the reference energy for the charged clusters.

Figure 4 shows that the geometry of the PES is similar in all three cases: the neutral, positively charged and negative cluster. We note rather significant differences in energy but in all cases we observe the valley of the lowest energies perpendicular to the Pd–Pd bond. The potential barrier for the hydrogen atom is 0.17 eV (3.92 kcal/mol), for the positively charged cluster the barrier is slightly higher, 0.5 eV (11.53 kcal/mol), but there is practically no barrier for the case of the negatively charged cluster.

Interaction of hydrogen with nickel clusters. The energy surface for the hydrogen atom interacting with the planar Ni_5 cluster is shown in Figure 5, in the upper part. There are significant differences between the PES geometry for nickel and palladium. The H atom binding energy is much higher for the Ni surface. The energy minimum –11.1 eV (–256 kcal/mol) appears at the position *4-fold hollow* at the edge of the cell. At the centre of the Ni–Ni bond (*bridge*) the binding energy is –10.4 eV

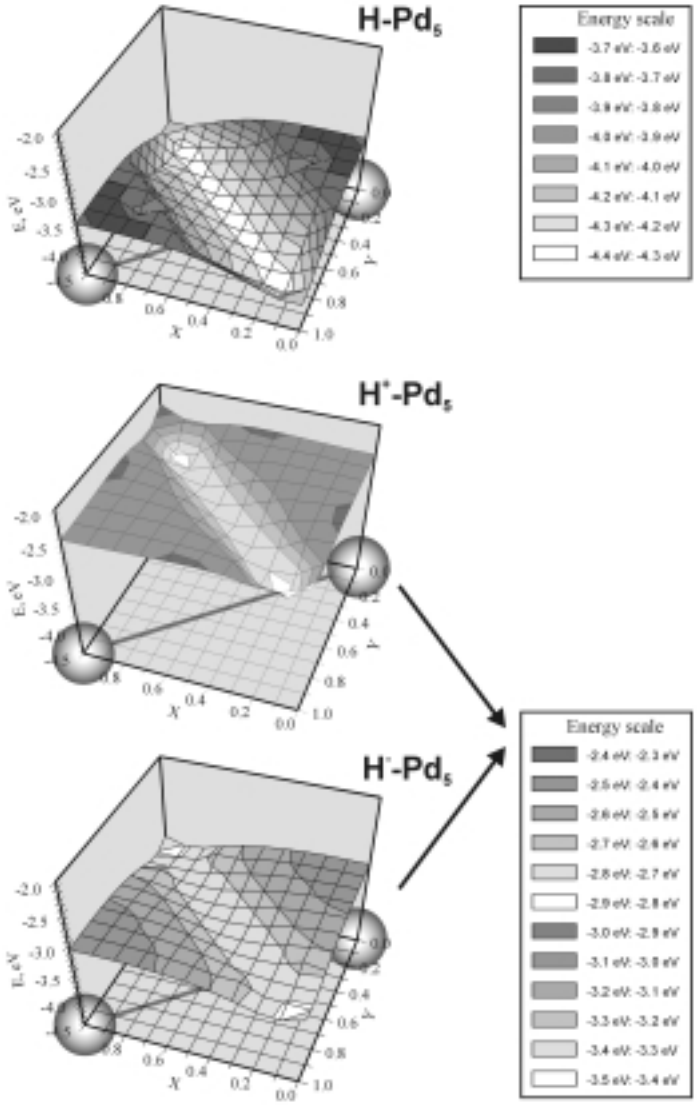

Figure 4. Energy surfaces for H atom binding energy in different positions over the upper right quarter of the Pd surface elementary cell. The calculations have been performed for the electrically neutral cluster (upper figure), the positively charged cluster H^+Pd_5 (medium figure) and the negatively charged cluster H^-Pd_5 (lower figure).

(–240.3 kcal/mol). The possible path for the hydrogen migration is perpendicular to the Ni–Ni bond and halves the bond. The plot of the PES crossection along the line (Y = 1-X) is shown in Figure 11. In contrast with the Pd case, the maximum appears at the *bridge* position. The energy barrier for motion along the line is 0.68 eV (15.60 kcal/mol).

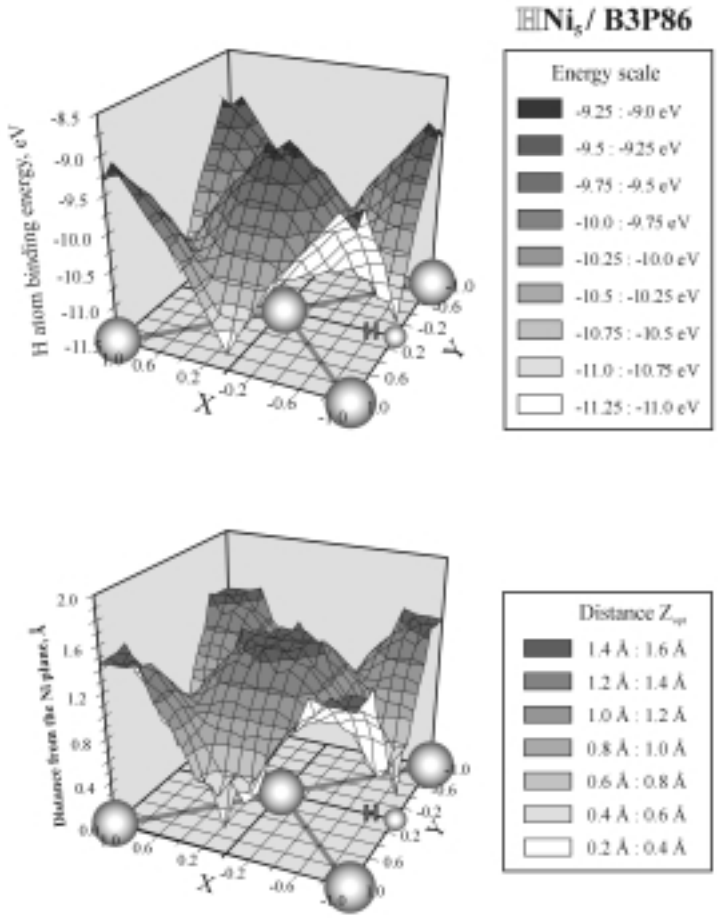

Figure 5. (Upper part) Three-dimensional plot of the binding energy of the single H atom in different positions over the elementary surface cell (fcc [100]) of nickel. (Lower part) A 3-D plot of the optimized distance of the H atom over the Ni cell, Z_{opt}. The unit on the X and Y axis is 1.762 Å.

The optimum distance of the hydrogen atom from the Ni surface is plotted in the lower part of Figure 5. The shortest distance to the surface, 0.2 Å, appears at the *4-fold hollow* position, at the energy minimum.

Figure 6 shows similar surfaces for the positively charged cluster, H^+Ni_5. The reference energy for the plot is assumed as the sum of energy of the isolated proton H^+ and the Ni_5 cluster. The geometry of the energy surface $E_b(X,Y)$ and the optimum distance surface $Z_{opt}(X,Y)$ are very similar in the neutral and charged case. It is interesting to note that the potential barrier is somewhat lower in the charged cluster case: 0.27 eV (6.23 kcal/mol). This suggests easier surface diffusion of proton than the neutral species.

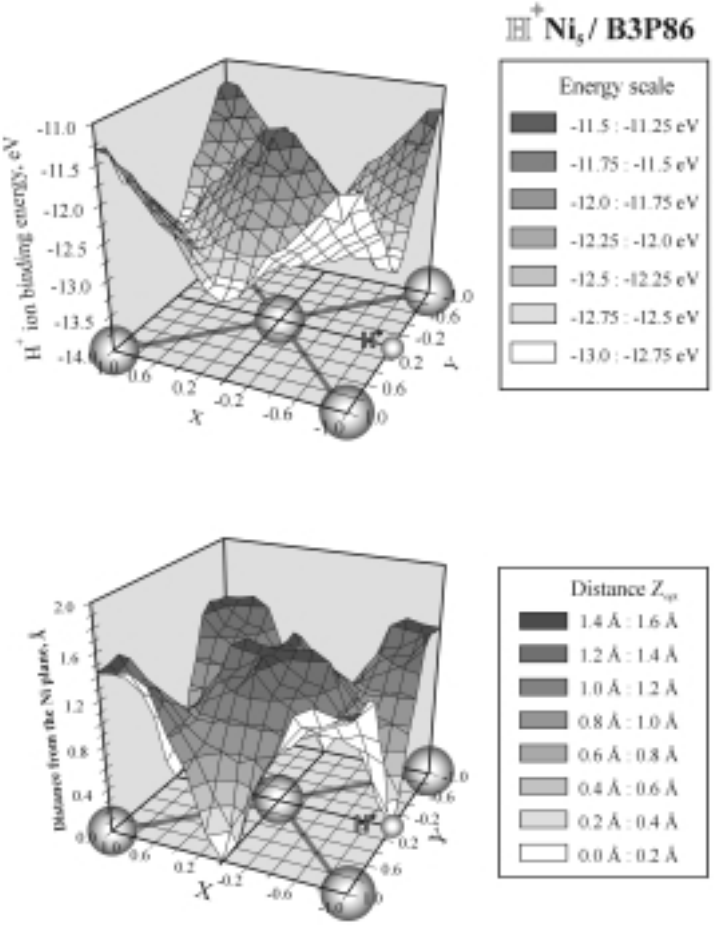

Figure 6. (Upper part) Three-dimensional plot of the binding energy of the proton H^+ in different positions over the elementary surface cell (fcc [100]) of nickel. (Lower part) A 3-D plot of the optimized distance of H^+ over the Ni cell, Z_{opt}. The unit on the X and Y axis is 1.762 Å.

Interaction of hydrogen with silver clusters. The energy surface for the hydrogen atom interacting with the planar Ag_5 cluster is shown in Figure 7, in the upper part. The geometrical shape of the PES for HAg_5 is closer to nickel than palladium while the numerical values of the binding energy are closer to the latter case. The energy minimum –2.85 eV (–65.7 kcal/mol) appears at the position *4-fold hollow* at the edge of the cell. At the centre of the Ag–Ag bond (*bridge*) the binding energy is –2.23 eV (–51.4 kcal/mol). The possible path for the hydrogen migration is perpendicular to the Ag–Ag bond and halves the bond (Y = 1-X). The maximum of the potential barrier appears at the *bridge* position. The energy barrier for the motion along the line is 0.62 eV (14.3 kcal/mol).

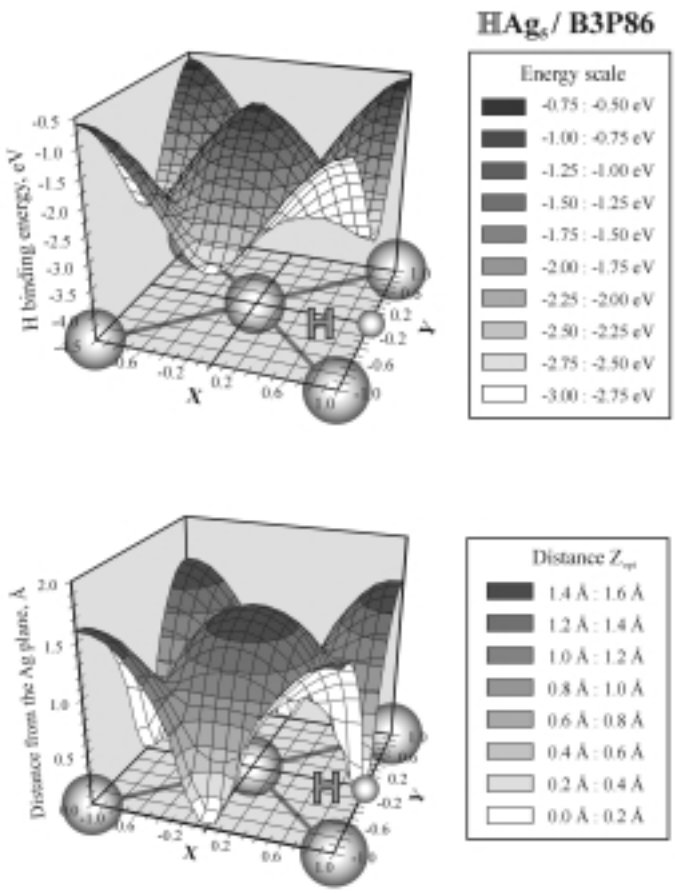

Figure 7. (Upper part) Three-dimensional plot of the binding energy of the single H atom in different positions over the elementary surface cell (fcc [100]) of silver. (Lower part) A 3-D plot of the optimized distance of the H atom over the Ag cell, Z_{opt}. The unit on the X and Y axis is 2.045 Å.

The optimum distance of the hydrogen atom from the Ag surface is plotted in the lower part of Figure 7. At the energy minimum (the *4-fold hollow* position) the hydrogen atom can be built in the metal plane – the optimum distance is 0 Å.

Figure 8 shows the energy and optimum distance surfaces for the positively charged cluster, H^+Ag_5. The reference energy for the plot is assumed as the sum of energy of the isolated hydrogen H and the Ag_5^+ cluster. At large distances between the H atom and the Ag plane the Mulliken partial charge on the hydrogen is very close to 0. Moreover, the reference energy of H and Ag_5^+ is by 7.05 eV lower than the value for H^+ and Ag_5. This might be connected with the spin states of the metal clusters: the Ag_5^+ state is assumed as the singlet and the Ag_5 is the doublet. The geometry of the energy surface $E_b(X,Y)$ and particularly the optimum distance plot $Z_{opt}(X,Y)$ are strikingly similar in the neutral and charged case. The barrier for the motion of the hydrogen on the charged cluster is very low: 0.35 eV (8.1 kcal/mol).

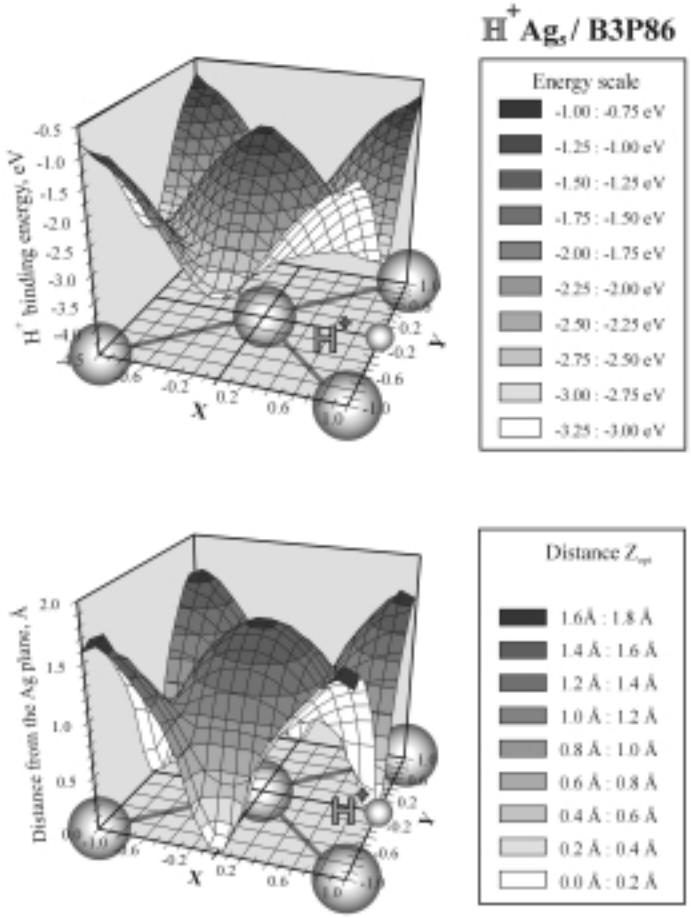

Figure 8. (Upper part) Three-dimensional plot of the binding energy of the proton H^+ in different positions over the elementary surface cell (fcc [100]) of silver. (Lower part) A 3-D plot of the optimized distance of H^+ over the Ag cell, Z_{opt}. The unit on the X and Y axis is 2.045 Å.

Interaction of hydrogen with copper clusters. The energy surface for the hydrogen atom interacting with the planar Cu_5 cluster is shown in Figure 9, in the upper part. The geometrical shape of the PES for HCu_5 is very similar to the HAg_5 case and the numerical values of the binding energy are of similar range. The energy minimum –3.39 eV (–78.2 kcal/mol) appears at the position *4-fold hollow* at the edge of the cell. At the centre of the Cu–Cu bond (*bridge*) the binding energy is –2.6 eV (–60.0 kcal/mol). The possible path for the hydrogen migration is perpendicular to the Cu–Cu bond and crosses the centre of the bond (Y = 1-X). The potential maximum appears at the *bridge* position. The energy barrier for the motion along the line is the highest of the four metals considered: 0.79 eV (18.2 kcal/mol).

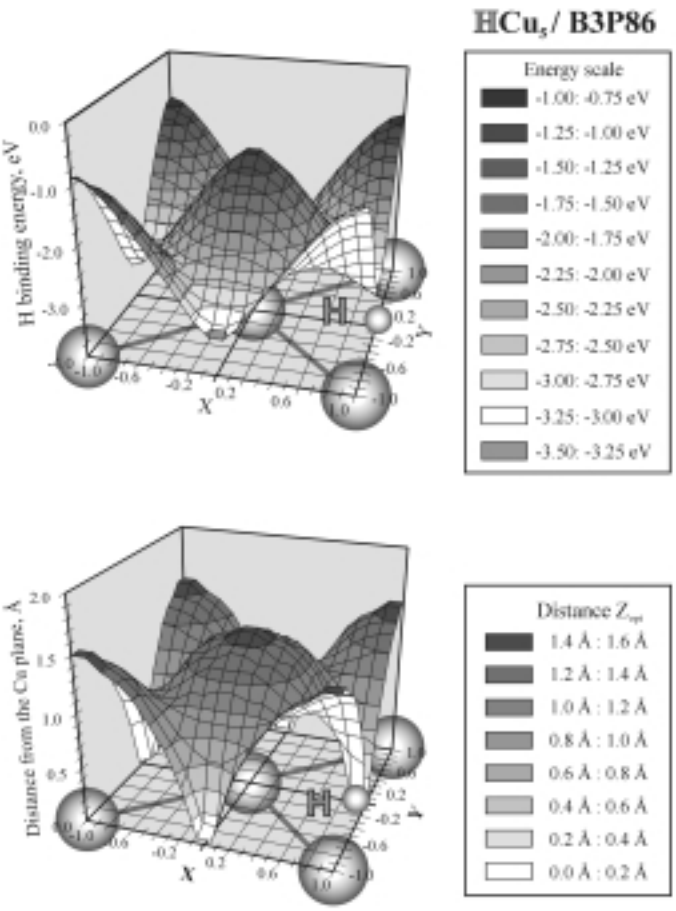

Figure 9. (Upper part) Three-dimensional plot of the binding energy of the single H atom in different positions over the elementary surface cell (fcc [100]) of copper. (Lower part) A 3-D plot of the optimized distance of the H atom over the Cu cell, Z_{opt}. The unit on the X and Y axis is 1.785 Å.

The optimum distance of the hydrogen atom from the Cu surface is plotted in the lower part of Figure 9. At the energy minimum (the *4-fold hollow* position) the hydrogen atom can be built in the metal plane – the optimum distance is 0 Å.

Figure 10 shows the energy and optimum distance surfaces for the positively charged cluster, H^+Cu_5. The reference energy for the plot is assumed as the sum of energy of the isolated hydrogen H and the Cu_5^+ cluster. At large distances between the H atom and the Cu plane the Mulliken partial charge on the hydrogen is very close to 0 and the reference energy of H and Cu_5^+ (the singlet) is by 6.88 eV lower than the value for H^+ and Cu_5 (the doublet). The geometry of the energy surface $E_b(X,Y)$ and particularly the optimum distance surface $Z_{opt}(X,Y)$ are very similar in the neutral and charged case. The barrier for hydrogen motion for the charged cluster is 0.58 eV (13.4 kcal/mol) and, like in the Ni and Ag cases, is lower than that for the neutral cluster.

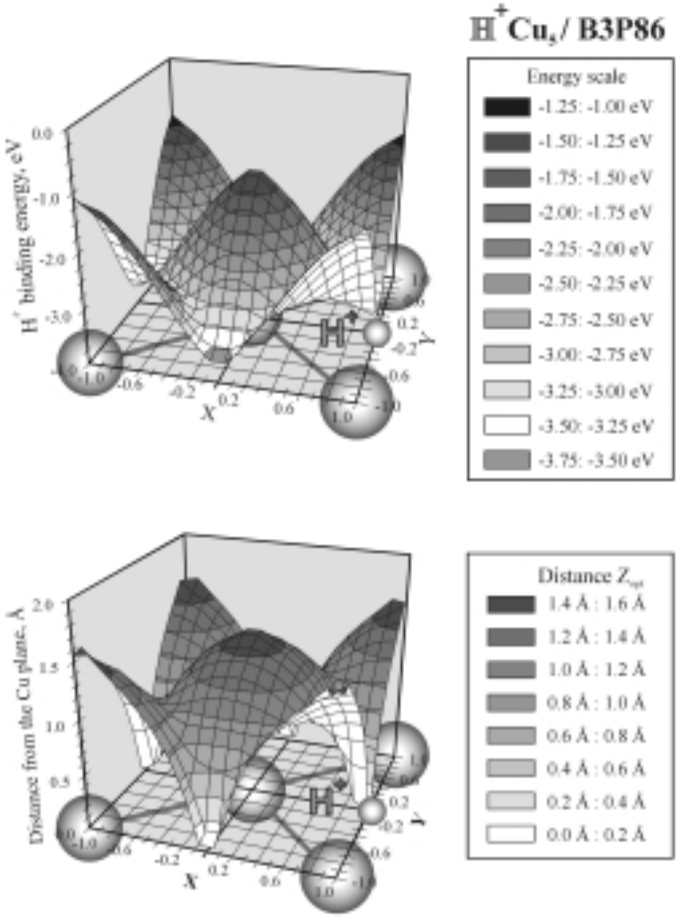

Figure 10. (Upper part) Three-dimensional plot of the binding energy of the proton H^+ in different positions over the elementary surface cell (fcc [100]) of copper. (Lower part) A 3-D plot of the optimized distance of H^+ over the Cu cell, Z_{opt}. The unit on the X and Y axis is 1.785 Å.

CONCLUSIONS

Figure 11 summarizes the results. The binding energy of the H atom along the crossection Y = 1-X is shown for all the metals considered: Pd, Ag, Cu and Ni. The former three curves correspond to the left ordinate scale, the latter to the right scale. The results of calculations suggest the possibility of easy diffusion of hydrogen atoms over the metal surface. The activation barriers are very low, from almost 0 to about 0.8 eV. The lowest barriers appear for Pd, in accordance with the experimental results, and suggest practically activationless movement of the hydrogen atom over the Pd surface. The barriers for Cu, Ag and Ni are within the range 0.6 to 0.8 eV. The result is of importance for understanding of chemical reactions proceeding at the metal

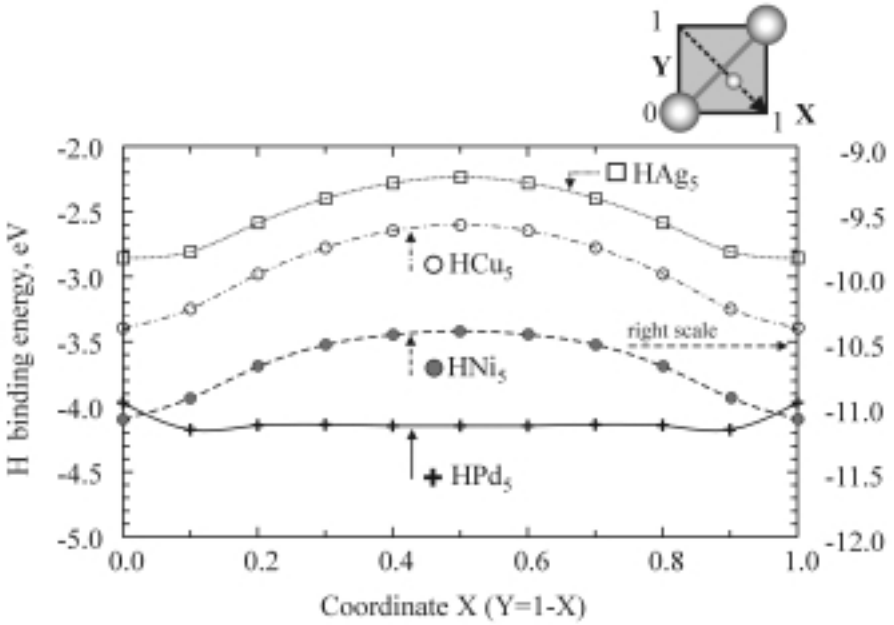

Figure 11. Comparison of the H atom binding energy along the direction Y = 1-X (perpendicular to the metal-metal bond) in the cells of Pd, Ni, Ag and Cu. The curves for Pd, Ag and Cu correspond to the left ordinate scale, the curve for Ni to the right scale.

surface, in particular the processes of heterogeneous catalysis on metals. The mobile hydrogen atom and, as it results from our preliminary calculations not reported in this paper, mobile oxygen atom, carbon monoxide molecule, hydroxyl radical, *etc.*, can easily move over the catalyst surface and react with other species, including larger, immobile molecules. It is worth noting that the diffusion processes proceed in quasi 2-dimensional space where the random encounter probability is much higher than in 3-dimensional space. This can in part explain the role of the metal catalyst in heterogeneous catalysis as a medium not only lowering the activation barriers for chemical reactions, but also a medium facilitating the probability of contact of reacting species.

Acknowledgment

The present work was supported by the Polish State Committee for Scientific Research (KBN grant nr 7 T09A 095 21).

REFERENCES

1. Yoshida S., Sakaki S. and Kobayashi H., Electronic Processes in Catalysis, Wiley-VCH, New York 1994.
2. Salahub D.R., in: Ab Initio Methods in Quantum Chemistry, vol. 2; Ed. Lawley K.P., Wiley, Chichester 1987, p. 447.
3. Truhlar D.G. and Morokuma K., Eds., Transition State Modeling for Catalysis, ACS Symposium Series vol. 215, American Chemical Society, Washington 1999.
4. Koch W. and Holthausen M.C., A Chemist's Guide to Density Functional Theory, Wiley-VCH, New York 2000.
5. Gross A., Theoretical Surface Science. A Microscopic Perspective, Springer, Berlin 2003.
6. Efremenko I., *J. Molecular Catal. A*, **173**, 19 (2001).
7. Paul J.-F. and Sautet P., *Phys. Rev. B*, **53**, 8015 (1996).
8. Løvvik O.M. and Olsen R.A., *Phys. Rev. B*, **58**, 10890 (1998).
9. Dong W. and Hafner J., *Phys. Rev. B*, **56**, 15396 (1997).
10. Ledentu V., Dong W. and Sautet P., *Surface Sci.*, **413**, 518 (1998).
11. Dong W., Kresse G. and Hafner J., *J. Mol. Catal. A*, **119**, 69 (1997).
12. Okuyama H., Siga W., Takagi N., Nishijima M. and Aruga T., *Surface Sci.*, **401**, 344 (1998).
13. Wonchoba S.E. and Truhlar D., *Phys. Rev. B*, **53**, 11222 (1996).
14. Mattsson T.R., Engberg U. and Wahnström G., *Phys. Rev. Lett.*, **71**, 2615 (1993).
15. Mattsson T.R., Wahnström G., Bengtsson L. and Hammer B., *Phys. Rev. B*, **56**, 2258 (1997).
16. Klinke D.E.J. and Broadbelt L.J., *Surf. Sci.*, **429**,169 (1999).
17. Lee A., Zhu X.D. and Deng L., *Phys. Rev. B*, **46**, 15472 (1992).
18. Lee A., Zhu X.D. and Deng L., *Phys. Rev. B*, **48**, 11256 (1993).
19. *Gaussian 98 (Revision A.9):* Frisch M.J., Trucks G.W., Schlegel H.B., Scuseria M.A., Robb M.A., Cheeseman J.R., Zakrzewski V.G., Montgomery J.A., Stratmann R.E., Burant J.C., Dapprich S., Millam J.M., Daniels A.D., Kudin K.N., Strain M.C., Farkas O., Tomasi J., Barone V., Cossi M., Cammi R., Menucci B., Pomelli C., Adamo C., Clifford S., Ochterski J., Petersson G.A., Ayala P.Y., Cui Q., Morokuma K., Malick D.K., Rabuck A.D., Raghavachari K., Foresman J.B., Cioslowski J., Ortiz J.V., Stefanov B.B., Liu G., Liashenko A., Piskorz P., Komaromi I., Gomperts R., Martin R.L., Fox D.J., Keith T.A., Al-Laham M.A., Peng C.Y., Nanayakkara A., Gonzalez C., Challacombe M., Gill P.M.W., Johnson B.G., Chen W., Wong M.W., Andres J.L., Head-Gordon M., Replogle E.S., Pople J.A., Gaussian Inc., Pittsburgh PA 1998.
20. Dunning T.H. and Hay P.J., in: Modern Theoretical Chemistry; Ed. Schaeffer III H.F., Plenum, New York 1976, p. 1.
21. Hay P.J. and Wadt W.R., *J. Chem. Phys.*, **82**, 270; 284; 299 (1985).
22. Alefeld G. and Volkl J., Eds., Hydrogen in Metals, vols. I, II, Springer, Berlin 1978.